Hindawi
Advances in Polymer Technology
Volume 2019, Article ID 8074626, 11 pages
https://doi.org/10.1155/2019/8074626

Research Article

Polymer Concentration and Solvent Variation Correlation with the Morphology and Water Filtration Analysis of Polyether Sulfone Microfiltration Membrane

Muhammad Azeem U. R. Alvi,[1] Muhammad Waqas Khalid,[1] Nasir M. Ahmad,[2] Muhammad Bilal K. Niazi,[2] Muhammad Nabeel Anwar,[1] Mehwish Batool,[3] Waqas Cheema,[2] and Sikandar Rafiq[4]

[1]*School of Mechanical and Manufacturing Engineering, Department of Biomedical Engineering and Sciences, National University Of Sciences and Technology, Islamabad, 44000, Pakistan*
[2]*School of Chemical and Materials Engineering, National University of Sciences and Technology, Islamabad, 44000, Pakistan*
[3]*Department of Chemical Engineering, COMSATS University Islamabad, Lahore Campus, 54000, Pakistan*
[4]*Department of Chemical Polymer & Composite Material Engineering, University of Engineering & Technology, Kala Shah Kaku Campus, Pakistan*

Correspondence should be addressed to Nasir M. Ahmad; nasir.ahmad@scme.nust.edu.pk

Received 13 November 2018; Revised 22 January 2019; Accepted 28 January 2019; Published 3 March 2019

Academic Editor: Haiqing Lin

Microfiltration flat sheet membranes of polyether sulfone (PES) were fabricated by incorporating varying concentrations of polymer and investigated the influence of substituting solvents. The membranes were prepared via immersion precipitation method. Different solvents that included NMP (N-methyl-2-pyrrolidone), DMF (dimethylformamide), and THF (tetrahydrofuran) were used to analyse their effect on the performance and morphology of the prepared membranes. Two different coagulation bath temperatures were used to investigate the kinetics of membrane formation and subsequent effect on membrane performance. The maximum water flux of 141 ml/cm^2.h was observed using 21% of PES concentration in NMP + THF cosolvent system. The highest tensile strength of 29.15 MPa was observed using membrane prepared with 21% PES concentration in NMP as solvent and coagulation bath temperature of 25°C. The highest hydraulic membrane resistance was reported for membrane prepared with 21% PES concentration in NMP as solvent. Moreover, the lowest contact angle of 67° was observed for membrane prepared with 15% of PES concentration in NMP as solvent with coagulation bath temperature of 28°C. Furthermore, the Hansen solubility parameter was used to study the effect on the thermodynamics of membrane formation and found to be in good correlation with experimental observation and approach in the present work.

1. Introduction

Drinkable water resources are declining every year leading to exploring viable options for water reusability to treat and purify it [1]. Membrane technology is extensively used worldwide among various techniques to purify water [2]. Microfiltration membranes are considered economical for water treatment to reduce the microbial and colloidal sources in water [3]. These membranes are pressure driven membranes and can also be used as pretreatment for reverse osmosis and nanofiltration water purification processes [1, 3]. Microfiltration membranes typically have a pore size ranging from 0.1 to 10 μm in size. These membranes are able to separate out bacteria and suspended particles [4] as well as macromolecules with a molecular weight less than 100,000 g/mole [5].

For the preparation of microfiltration membranes, different polymers are used commercially such as polyvinylidene fluoride, polyvinyl alcohol, chitosan, polyvinyl chloride, polyacrylonitrile, polypropylene, polyvinyl alcohol,

polyimide, cellulose acetate, and polyether sulfone (PES) [6]. All these polymers are used for their various characteristics. For a specific polymer to be useful, it must possess various characteristics such as excellent high heat aging resistance, good mechanical properties, and environment durability [7]. Polyethersulfone (PES) is one of the most commonly used polymers for fabrication of microfiltration membrane. PES is an amorphous thermoplastic polymer and has the highest number of moieties in the polymer repeating unit in the sulfone group. Hence, the PES is the most hydrophilic in the sulfone group polymers [8]. Moreover, PES has high mechanical strength, stability at pH from 2 to 13 and chemical resistance, which makes it quite suitable to be used as membrane material [9, 10]. PES is soluble in aprotic polar solvents such as dimethylformamide (DMF), N-Methyl-2-pyrrolidone (NMP), etc. Furthermore, tetrahydrofuran (THF) [11] is borderline aprotic polar solvent and used as a cosolvent with NMP as main solvent [12].

An important advantage of asymmetric membranes is a dense skin layer with porous substructure. Skin layer offers selectivity and permeability, whereas the sublayer provides mechanical strength. Asymmetric polymeric membranes formed by immersion precipitation method are based on liquid-liquid phase separation [13–17]. It has been suggested that gelation is responsible for the formation of skin. Furthermore, porous sublayer is formed by liquid-liquid phase separation by growth and nucleation [13, 15, 18–22]. Thermodynamics and kinetics of membrane formation plays vital role in the morphology and performance of membranes [23]. Thermodynamics of membrane formation can be studied by Hansen solubility parameters (HSP) [24]. Thermodynamics require that the free energy of mixing must be zero or negative for the solution process to occur at the same time. The membrane formation depends on both solvent-nonsolvent and polymer-solvent demixing [25].

The kinetics of membrane formation can be controlled by temperature of coagulation bath [24]. The parameters such as polymer concentration [26], solvent [27], coagulation bath [28], conditions for preparation [29], polymer solution temperature, air moisture, and evaporation time before the wet phase have significant impact on the morphology and properties of the prepared membranes [30]. A change in one or more parameter leads to a change in the properties of the membrane as discussed elsewhere [31–33].

In consideration of the above, the present work is focused on the investigation of effect of polymer concentration variation and different solvents substitution in the dope solution used for the performance of flat sheet microfiltration membranes. The structure and properties such as tensile strength, flux, contact angle, and membrane hydraulic resistance of prepared membranes are analysed and correlated with the composition and concentration of polymer solution. Moreover, the Hansen solubility correlated parameters were used to study the thermodynamics and kinetics of the membrane formation.

2. Materials and Methods

2.1. Materials. Polyethersulfone, NMP, DMF, and THF were purchased from Sigma Aldrich. All the chemicals were used without further purification. Deionized water was used in the fabrication of membranes.

2.2. Preparation of Membranes. The flat sheet membranes were prepared by phase inversion method using casting machine. Five different formulations were prepared as shown in Table 1. PES was dissolved in respective solvent and stirred for 24 hours. The prepared solutions were casted at room temperature (23°C) on nonwoven polypropylene/polyethylene fabric Novatexx 2471, (Freudenberg Germany) placed on a glass plate. Solvent was applied on the support material before casting the polymer solution on the support material [35]. Casting was done by casting machine. Then the casted film was immersed in coagulation bath (25°C and 28°C) for 5 mins to let the demixing complete. After the formation of membranes, these were dried under ambient conditions and kept for characterization testing [36, 37]. The graphical abstract is shown in Figure 1.

2.3. Membrane Hydraulic Resistance (MHR). The MHR is the resistance of membrane to the feed flow. MHR is the indication of tolerance of membrane towards pressure and was calculated by [38]

$$R_m = \frac{\Delta P}{J_W} \tag{1}$$

where R_m is the membrane resistance (KPa $ml^{-1}cm^2h^1$), ΔP is the transmembrane pressure (KPa), and J_W is the water flux (ml $cm^{-2}h^{-1}$).

2.4. Fourier Transform Infrared Spectroscopy (FTIR). Bruker Alpha ATR spectrometer was used for IR characterization of the membranes. FTIR was carried out to investigate the change in functional groups of formulated membranes using different solvents and variations in polymer concentration. All the samples were tested in their natural state using ATR. The samples were cut into 1 x 0.5 cm in dimension and placed on the IR window.

2.5. Contact Angle Analysis. The contact angle was measured by sessile drop measurement technique to determine the extent of hydrophilicity or hydrophobicity of the formulated membranes. Typically, 5μL drop of distilled water was placed on the surface with a needle tip. A magnified image of the drop was then taken with a digital camera; static contact angle of the droplet was calculated using ImageJ LBADSA (Low-Bond Axisymmetric Drop Shape Analysis) software in degrees. The reported data was average of four determinations at different points on the prepared membrane and then mean and standard deviation were calculated.

2.6. Mechanical Testing. Mechanical testing was carried out for the prepared membranes according to the standard ASTM

Table 1: Composition of prepared membranes.

Serial No.	Membrane Codes	Polyether sulfone Concentration (Wt %)	Solvents
1.	M1	15 %	NMP
2.	M2	18 %	NMP
3.	M3	21 %	NMP
4.	MS-1	21 %	DMF
5.	MS-2	21 %	70% NMP, 30% THF.

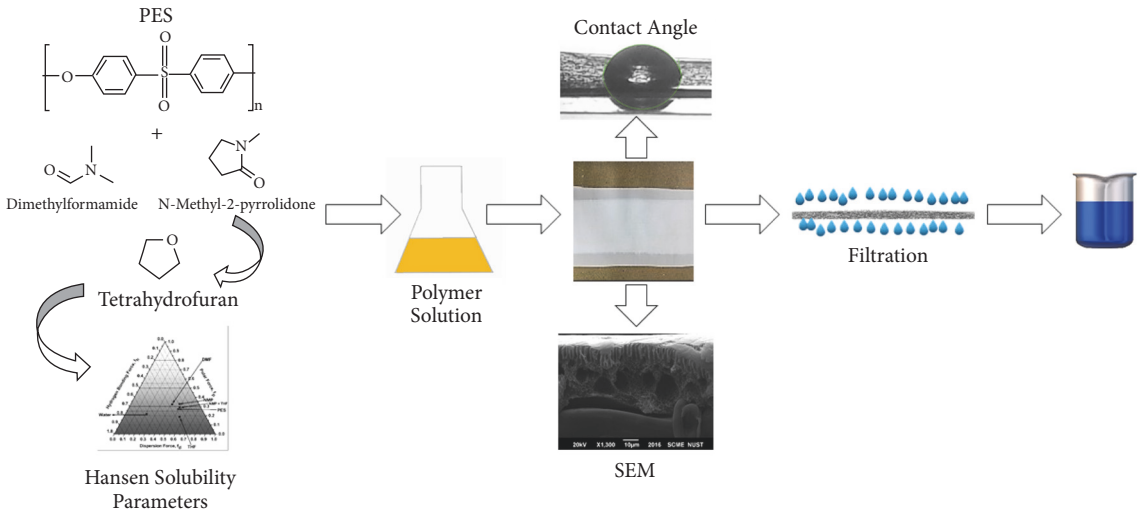

Figure 1: Graphical abstract.

D882. The tensile properties of the membranes were determined using Trapezium-X Universal testing machine (AG-20KNXD Plus Shimadzu corporation, Japan). The maximum load limit was 20kN. The strain rate was 3mm/sec. The gauge length of the samples was 2 cm, while the total sample length was 7 cm. The width of the samples was 1.1 cm and thickness was 0.03 cm.

All the samples were tested at room temperature. The mechanical testing was performed to evaluate the effect of polymer concentration increment and solvent variation on the prepared membranes.

2.7. Scanning Electron Microscopy. The topographical and cross-sectional morphologies of membranes were studied by scanning electron microscopy (JOEL JSM-6490A Analytical scanning electron microscope Japan). Membranes were cut into 0.25cm^2 samples. For cross-sectional morphology, these were immersed in liquid nitrogen for approximately 60 seconds to freeze. After freezing, the membranes were broken into smaller fragments to perform SEM of cross section. The samples were gold coated using JFC-1500 Ion sputtering unit.

2.8. Pure Water Flux. Filtration cell was used to test the permeation characteristics of the fabricated membranes at different pressures of 26.66, 39.99, 53.32, 66.66, and 79.99 kPa for determination of water flux. For this purpose, filtration equipment was attached to a vacuum pump with adjustable pressure gauge to obtain desirable pressure to permeate the water through the prepared porous membranes. For each experiment, 20 ml of water was taken in the fritted glass funnel and then pressure was applied by the vacuum pump to permeate the water through the membrane placed on glass support base. Flux was calculated using the equation

$$J = \frac{v}{a.t} \quad (2)$$

where v is the volume of water, a is the effective membrane area, and t is the permeation time.

2.9. Hansen Solubility Parameter (HSP). HSP is valuable in explaining the influence of parameters such as polymer, solvents, and nonsolvent on membrane preparation. The thermodynamics and kinetics of the membrane fabrication must be considered to explain the fabrication process and its relation to the membrane performance. The thermodynamics

mainly depend on the chemical potential of the process parameters [39]. Therefore, the HSP can be an important tool to discuss their influence on the membrane structure formation [40]. The solubility parameter of polymer and solvent by Hansen solubility parameter can be defined as

$$\delta_t = \sqrt{\delta_d{}^2 + \delta_p{}^2 + \delta_h{}^2} \tag{3}$$

where δ_t is Hansen solubility parameter, δ_d is energy from the dispersion bonds, $\delta_p$is energy from dipolar intermolecular forces, and δ_h is the energy from the hydrogen bonds.

The polymer solvent interaction can be defined as

$$\Delta\delta_{p-s} = \sqrt{\left((\delta_{D,P} - \delta_{D,S})^2 + (\delta_{P,P} - \delta_{P,S})^2 + (\delta_{H,P} - \delta_{H,S})^2\right.} \tag{4}$$

Polymer and nonsolvent interaction is given by

$$\Delta\delta_{P-NS} = \sqrt{(\delta_{D,P} - \delta_{D,NS})^2 + (\delta_{P,P} - \delta_{P,NS})^2 + (\delta_{H,P} - \delta_{H,NS})^2} \tag{5}$$

Solvent and nonsolvent is given by

$$\Delta\delta_{S-NS} = \sqrt{(\delta_{D,S} - \delta_{D,NS})^2 + (\delta_{P,S} - \delta_{P,NS})^2 + (\delta_{H,S} - \delta_{H,NS})^2} \tag{6}$$

The calculations based on these relations can be used to predict and understand the membrane structure formation [41]. The Hansen solubility parameter values of polymer, solvent, nonsolvent, and their interaction with each other are given in Table 2.

Fractional parameters were derived from the Hansen parameters using the equations

$$f_d = \frac{\delta_D}{(\delta_D + \delta_P + \delta_H)} \tag{7}$$

$$f_p = \frac{\delta_P}{(\delta_D + \delta_P + \delta_H)} \tag{8}$$

$$f_h = \frac{\delta_H}{(\delta_D + \delta_P + \delta_H)} \tag{9}$$

The sum of three fractional parameters remains equal to 1.

$$f_d + f_p + f_h = 1.0 \tag{10}$$

3. Results and Discussion

3.1. Fourier Transform Infrared Spectroscopy. The ATR-FTIR spectra of the formulated membranes are shown in Figure 2. The strong peak of C_6H_6 benzene ring stretch at 1587 cm^{-1} is the aromatic band of polyethersulfone [42]. The sharp peak at 1147 cm^{-1} is due to S=O group symmetric stretching vibration [43]. The peak at 1476 cm^{-1} is the representative band of C-S stretch [44]. The peak around 1240 cm^{-1} is due to C=C stretching [45]. The M1, M2, and M3 membranes have shown no effect on FTIR spectra. There is a difference in the spectra of membranes with solvent variation, i.e., MS-1 and MS-2.

Figure 2(b) has the spectra of polyethersulfone with NMP, DMF, and cosolvent system of NMP+THF. The shift at 2931 cm^{-1} is due to symmetric methyl C-H bond stretching in membrane with DMF [46]. It is attributed to the presence of residual solvent [47]. While the peaks in the region of 2839 and 2931 cm^{-1} of membranes with cosolvent system are due to the presence of C-H stretching vibrations of THF [48].

3.2. Morphological Analyses. Scanning Electron Microscopy (SEM) was used to understand the effect of variability in polymer and solvent substitution on the morphology of the prepared membranes. Figure 3 represent the cross-sectional and surface images of the membranes. In membranes prepared with PES variation, a marked difference between the structures was observed. The M1 membrane was found to be more porous than M2 and M3 formulated membranes. Similarly, the M1 membrane appeared to have thin structures with cross-sectional length of 14.898 μm. The support layer appears to be thinner than the others. This can be attributed to the temperature of coagulation bath, whereas a thick structure of the membrane was observed in M3 membrane after change in the thermodynamics of casting solution and coagulation bath temperature.

Similarly, a change in structure was recorded when the membranes were prepared with solvent substitution. In MS-1 membrane, macrovoids were observed in the cross section. The underlying structure of the membrane can be attributed to high demixing rate of DMF [38, 49]. In MS-2 formulated membrane, the active layer structure was found to be large. A persistent increase in flux rate was observed with increasing pressure for this membrane [50]. In Figure 3(a) the structure of the membrane appears to be thin, whereas in Figures 3(b) and 3(c) the thickness of the prepared membranes appears to increase with increase in polymer concentration. The surface images of the membranes appear to be rough.

3.3. Contact Angle Analysis. The contact angle of the fabricated membranes was analysed using Low-Bond Axisymmetric Drop Shape Analysis (LBADSA) of surface contact angle of sessile drop based on Young-Laplace equation. The LBADSA offers first-order approximation solution to the Young-Laplace equation. This method was used as a plugin on ImageJ software [51]. The capillary forces were the only driving force for the small droplet. Drop-base diameter defined the spatial resolution of the sessile drop measurement.

Figure 4 represents the contact angle of the fabricated membranes. It was observed that with the membranes prepared by changing the concentration of polymer (M1, M2, and M3 membranes) the surface became more hydrophobic as the concentration of polymer increased [52]. This can be attributed to the fact that the hydrophilicity of the formulated membrane depends on the pore size and porosity. The flux results clearly indicate the trend of hydrophilicity

Table 2: Hansen solubility parameter values of polymer, solvent, nonsolvent, and their interaction [34].

S, P, NS.	Dispersion Parameter (δ_d) $(MPa)^{0.5}$	Polar Parameter (δ_p) $(MPa)^{0.5}$	Hydrogen Bonding Parameter (δ_h) $(MPa)^{0.5}$	Total Solubility Parameter (δ_T) $(MPa)^{0.5}$	Polymer Solvent Interaction ($\delta_{P\text{-}S}$) $(MPa)^{0.5}$	Polymer-Non-Solvent Interaction ($\delta_{P\text{-}NS}$) $(MPa)^{0.5}$	Solvent-Non-Solvent Interaction ($\delta_{S\text{-}NS}$) $(MPa)^{0.5}$
NMP	18.0	12.3	7.2	22.9	2.96	-	35.37
DMF	17.4	13.7	11.3	24.8	4.20	-	31.13
THF	16.8	5.7	8.0	19.4	5.94	-	35.83
NMP +THF				21.85	2.68		35.38
PES	19.6	10.8	9.2	24.19	-	-	-
WATER	15.6	16.0	42.3	47.8	-	33.74	-

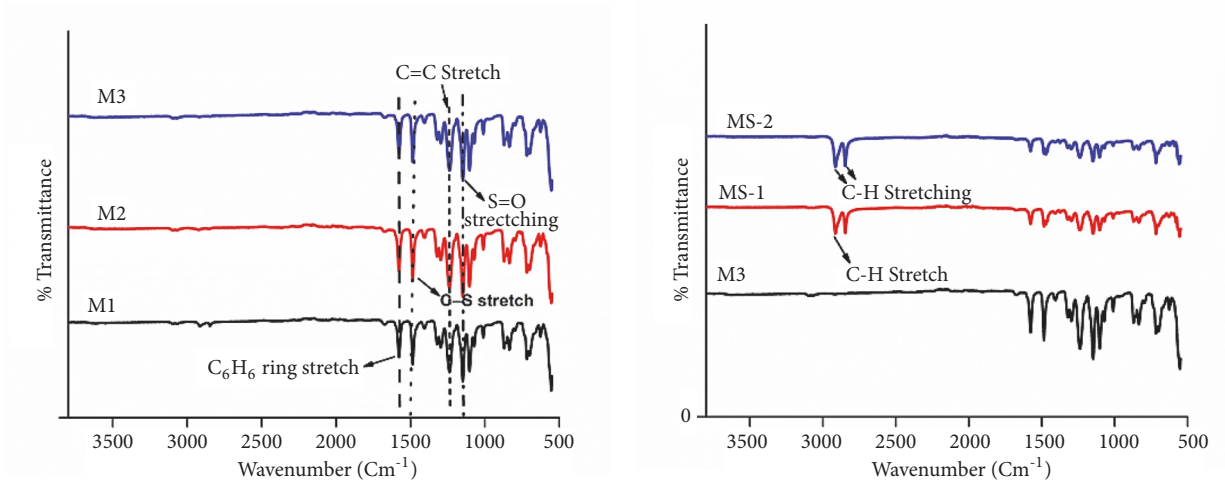

Figure 2: ATR-FTIR spectra of membranes prepared by (a) polymer concentration variation and (b) membranes prepared by solvent variation.

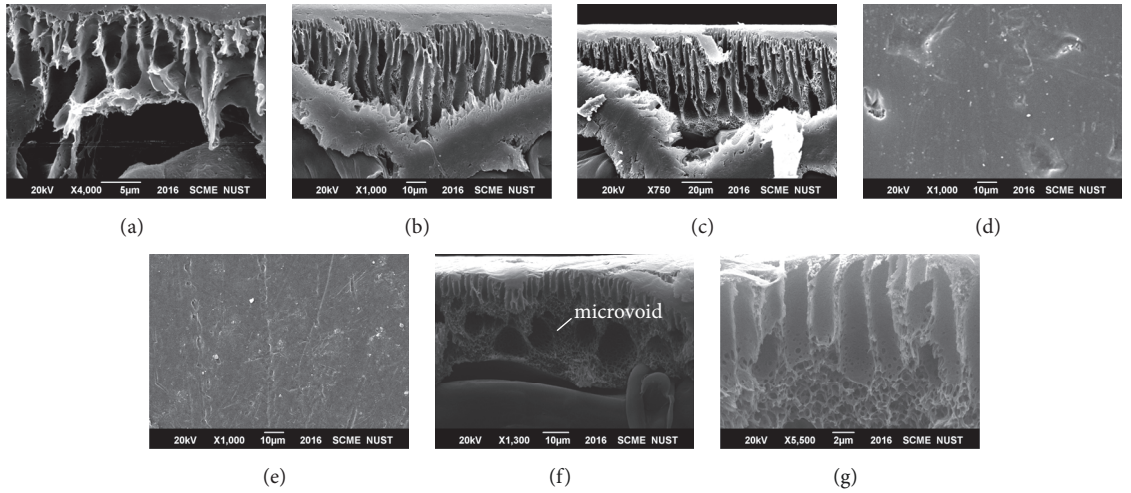

Figure 3: SEM Images. (a) M1 cross-sectional, (b) M2, (c) M3 cross-sectional, (d) M1 Surface, (e) M3 Surface, (f) MS-1, and (g) MS-2.

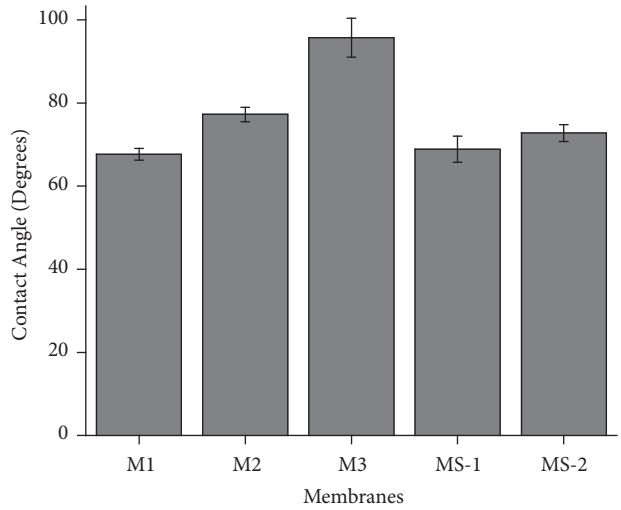

Figure 4: Contact angle of formulated membranes analysed by ImageJ. Error bars represent standard deviation and five measurements were recorded for contact angle.

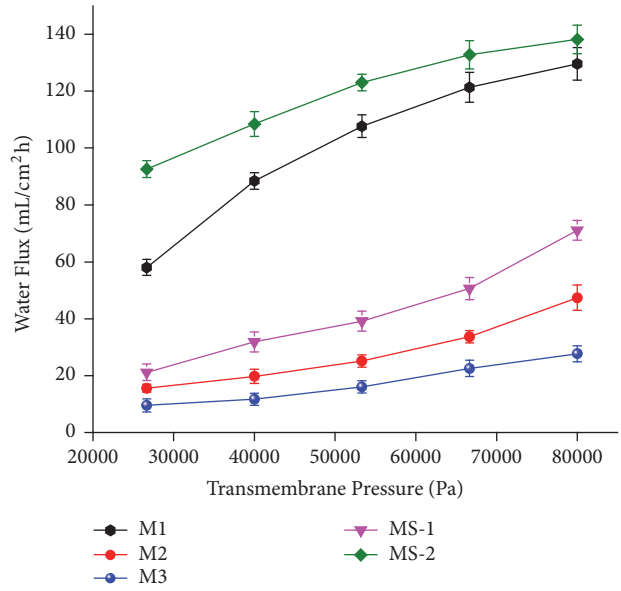

Figure 5: Water flux of membranes prepared by polymer concentration variation and solvent variation.

in the formulated membranes [45], whereas the contact angle was observed to decrease with change of solvents in formulated membranes (MS-1 and MS-2), as compared to M1 formulated membrane. This can be explained by Hansen solubility parameters, such as faster demixing rate in MS-1 which resulted in porous structure, hence hydrophilicity, whereas, in MS-2, the $\delta_{P\text{-}S}$ value dropped to 2.68 $MPa^{1/2}$. This resulted in relatively less thermodynamically stable solution and better demixing leading to porosity on surface [53].

3.4. Water Flux Analyses. The water flux of all the membranes was measured to determine their water permeability. All the membranes were tested for water flux at different pressures under steady state conditions. The water flux has a direct relation to the porosity of the top layer including the number of pores and their size [54]. Figure 5 represents the pure water flux of the formulated membranes recorded at different pressures, with at least 4 determinations of each pressure.

The M1 membrane had high values of water flux. Results were supported by SEM analysis as seen in Figure 5. The sublayer channels were smaller than the membrane with highest level of PES, i.e., M3 using NMP as solvent. The underlying channel system aided the flow of water through the membrane at a faster rate. Moreover, the increase of pressure also influenced the water flux. However, the permeability of the membrane also increased due to underlying morphology of the membranes.

Furthermore, the pure water flux reduced with increase in concentration of polymer in prepared membranes. It can be attributed to increase in thickness and formation of dense skin layer with increase in polymer concentration. Similarly, the productivity of the formulated membrane for liquid separation also decreased [55]. On the other hand, the dilute polymer solution formed a thin and porous skin layer with increased values of flux at different pressures as evident from SEM analyses.

By increasing the concentration of polymer, the viscosity of the polymer solution increased, and the coagulation was slowed down due to strong interaction of solvent and polymer. Moreover, it also resulted in molecules aggregation of polymer because the interaction of polymer and water as nonsolvent was higher. As a consequence, it decreased the dissolving capacity of polymer for solvent [56]. The membrane with high polymer concentration and high viscosity can slow down the diffusional exchange rate of NMP and water in the sublayer structure of the membrane. This resulted in the slowdown of the precipitation rate at the sublayer level [57].

For M1 formulated membrane, high flux rate was observed in membranes prepared with PES concentration variation. This may be attributed to decrease in the thickness of surface during polymer-rich phase [40].

Meanwhile, in MS-1 formulated membrane the pure water flux was observed to be higher than the M3 membrane as the top skin of the membrane was even thinner. SEM image analysis shows similar structure. This can be attributed to the volatile nature of the THF. During dry phase the THF on the surface of the casted membrane was evaporated forming more porous structure. The MS-1 formulated membrane had higher water flux values then the M3 membrane. The presence of DMF in the cast solution facilitated the formation of pores on the membrane surface. After immersion in the nonsolvent bath the formation of more porous structure was facilitated [35, 40, 58, 59].

3.5. Mechanical Strength. The tensile strengths of the formulated membranes with different concentrations and solvents were investigated. Figure 6 represents the tensile strength, elongation at break, and modulus of the formulated membranes. As the concentration of polymer was increased, the tensile strength of the membranes also improved. This may

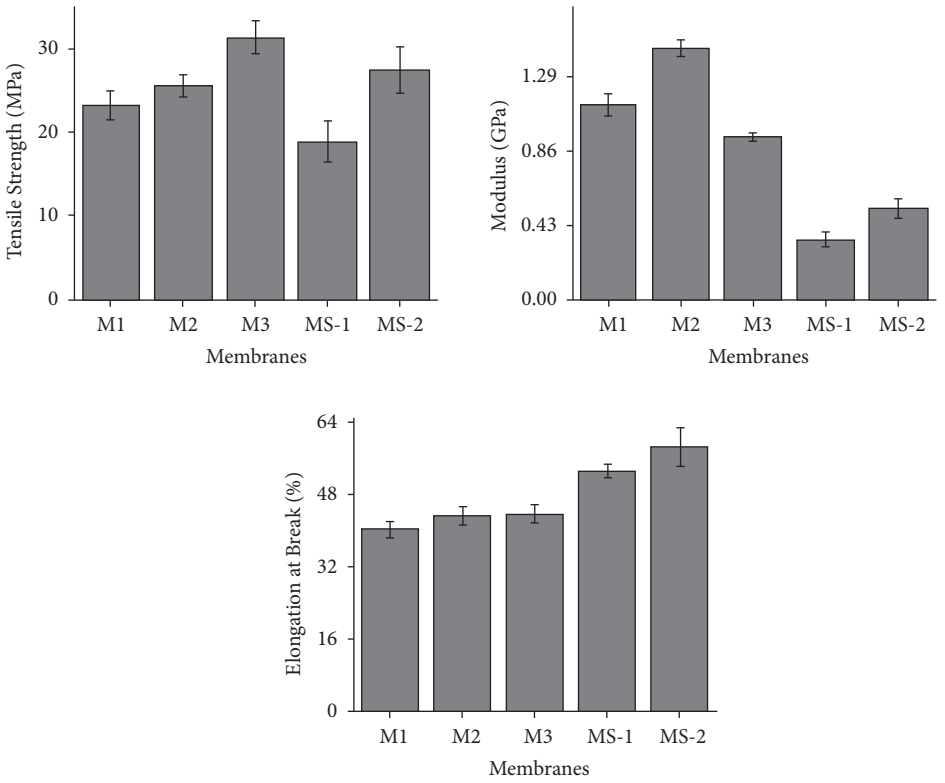

Figure 6: Tensile strength, elongation at break, and modulus of prepared membranes.

be due to the increase in the thickness of the top layer by enhancing the concentration of the polymer, Meanwhile, with the membrane prepared by DMF as solvent, the tensile strength of the membrane decreased as compared to M3. This can be attributed to the decrease in thickness of the top layer of the membrane due to difference of hydrogen bonding value of 11.3 $MPa^{1/2}$ resulting in faster diffusion rate of solvent into nonsolvent [38]. However, the tensile strength increased when NMP+THF was used as a solvent in formulated membrane as compared to DMF. This can be associated with miscibility of NMP with water. There is a reduction in thickness of membrane prepared by DMF and PES. This can be explained by the fact that the transport of NS in the polymer solution was slower than transport of DMF into water. Results showed that the tensile strength is directly proportional to the concentration of polymer in formulated membrane [60]. According to Hansen solubility parameter, the solvent-nonsolvent interaction of $\Delta\delta_{DMF-WATER}$ is 31.13 $MPa^{1/2}$, which is less than other solvents used. The more miscibility of DMF and nonsolvent allowed rapid demixing and disturbance in the thermodynamics of the stable casted solution. This resulted in formation of thin layer on top, subsequently decreasing the tensile properties of the membrane [61].

3.6. Membrane Hydraulic Resistance (MHR). MHR is inversely proportional to the permeate flux of the membrane. MHR was observed at five different pressures. Figure 7 shows the membrane hydraulic resistance of the formulated membranes. Membrane hydraulic resistance was measured by the inverse of the slopes of the pure water flux against pressure linear dependences. MHR is used to determine the intrinsic resistance of formulated membrane against the water feed. The results indicate that the M3 had the highest MHR measured at all the pressures. It can be explained by the fact that the MHR is inversely proportional to the flux and a lowest flux was recorded for M3 membrane at

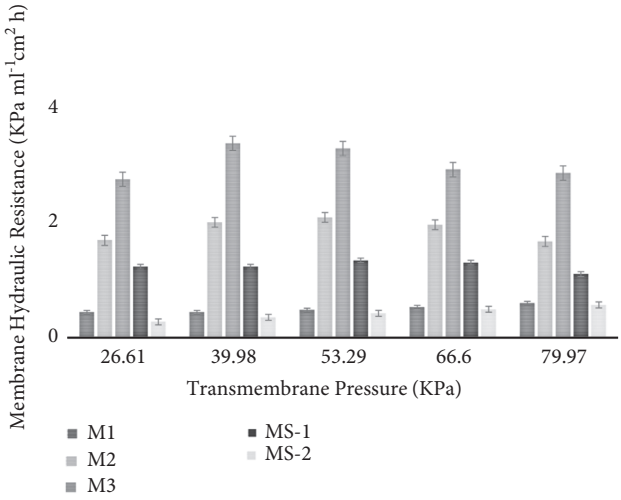

Figure 7: Membrane hydraulic resistance of prepared membranes measured at different pressures.

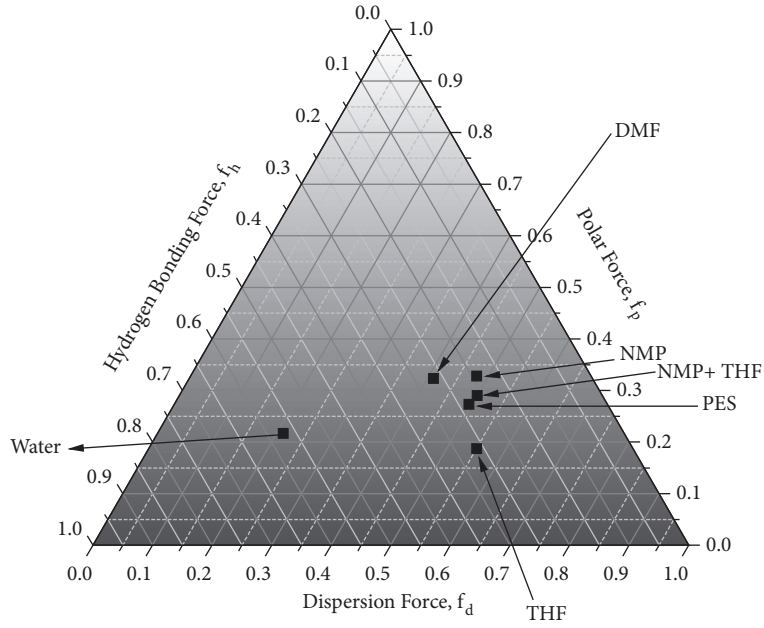

Figure 8: Teas graph of solubility parameter interaction of polymer, solvent, and nonsolvent.

all the pressures. Moreover, the reason for low flux rate can be attributed to the structure of the formulated membrane. For membranes prepared with solvent variation (MS-1 and MS-2), the MS-1 membrane was found to have good intrinsic resistance because of higher values of MHR calculated [38].

3.7. Correlation with Polymer Concentration. Three membranes (M1, M2, and M3) were used to observe the influence of polymer concentration. NMP was used as a solvent (S) in the formulations. The pure water flux data of the membranes was used to evaluate the effect of polymer concentration on membranes performance [62]. The M1 membrane had the highest flux values studied at various pressures. As the polymer concentration was increased, the top layer of the membrane became less porous as indicated by SEM analysis. Moreover, the solution became thermodynamically stable with increase in concentration of PES. As a result, the phase separation slowed down [63].

According to solubility parameter values, the affinity of NMP for nonsolvent (NS) was higher than the affinity of PES for NS. Therefore, the difference in affinities resulted in thermodynamic instability and membrane of the type M1, resulted in thinner upper surface as evident in SEM analysis, subsequently more porous surface.

The pore size of the membrane was reduced with increase in polymer concentration. This resulted in low water permeability through membrane. The M3 membrane had the lowest pure water flux. It can be explained by the fact that the phase separation of PES depends on the thermodynamic and kinetic factors of polymer, solvent, and nonsolvent. In the fabrication of M1 and M2, the temperature of coagulant bath was 28°C, whereas M3 membrane was casted at a temperature of 25°C. It was observed that the coagulant bath temperature controls the S-NS phase of the membrane fabrication. The exchange of S-NS increased at 28°C, as previous findings support this temperature variation explanation [64]. The polymer-solvent interaction value of 2.96 $MPa^{1/2}$ suggests better miscibility, leading to delayed demixing of solvent in nonsolvent. The pores on upper surface of the membrane directly affect the water permeation across the membrane [24].

3.8. Correlation with Solvent Variation. The solvents variation was investigated and compared with M3 membrane. The concentration of PES was kept constant at 21%. The M3 formulated membrane performance in terms of pure water flux was found to be the lowest among the other two formulated membranes M1 and M2. The temperature of water bath used for all formulated membranes in this part was 25°C. In this study, the performance of MS-1 and MS-2 in terms of pure water flux and contact angle was observed to improve.

The kinetics of the phase inversion also influenced the fabrication of membranes and the interaction of solvents and nonsolvent during the wet phase, which was the polymer poor phase, while the temperature of coagulation bath had effect on rapid and delayed demixing rates, as both had effects on the morphology of the resulting membranes. When the demixing rate was high, the MS-1 membrane with thin skin layer was formed. The reason for this can be explained from the $\delta_{S\text{-}NS}$ value of 31.13 $MPa^{1/2}$. This can be attributed to high affinity of DMF towards NS (water) with strong hydrogen bonding parameter, whereas the demixing rate was slower in MS-1 membrane because of high value of $\delta_{S\text{-}NS}$, i.e., 35.38 $MPa^{1/2}$. It is interesting to note that the $\delta_{P\text{-}S}$ value for cosolvent in MS-2 membrane decreased to 2.68 $MPa^{1/2}$ [24]. Teas graph in Figure 8 was used to observe the relative positions of polymer, solvents, and nonsolvent. Teas graph provides theoretical explanation of the solubility of polymer,

solvent, and nonsolvent with each other. Teas graph translates polar, hydrogen, and dispersion components into a two-dimensional graph [34].

4. Conclusions

Polyether sulfone microfiltration membranes were prepared by phase inversion method. Moreover, morphology and performance were correlated with polymer and solvent variation from the consideration of Hansen solubility parameters. The temperature of coagulation bath had effects on the performance and morphology of prepared membranes. In polymer concentration correlation, the concentration increase was found to have a negative effect with decreasing flux, whereas positive effects of tensile strength enhancements were observed. Moreover, in solvent variations correlation, the different demixing rate of solvents in nonsolvent affected the performance of the membranes. The prepared membranes were investigated for their strength, contact angle, water permeability, surface chemistry, and morphology. Thermodynamics and kinetics of the membrane formation were also discussed. For this purpose, Hansen solubility parameters for the polymer, solvent, and nonsolvent were calculated. PES membrane prepared with 21% polymer concentration in NMP solvent was observed to undergo relatively less phase separation, hence resulting in less pores and less water flux. Low concentration of 15% PES in NMP resulted in relatively thin membrane but more pores resulting in higher water permeation across the membrane. The contact angle for the membrane prepared with 15% PES concentration was the lowest while with 21% PES concentration in NMP was found to exhibit the highest contact angle. The contact angle of membrane prepared with 15% PES concentration in NMP was found to be closer to the membrane prepared with 21% PES in DMF with values of 67° and 68°, respectively. Moreover, the membrane prepared with 21 % PES concentration in NMP and THF cosolvent the contact angle was slightly higher than two abovementioned membranes. The water flux of membrane prepared with 21% PES concentration in NMP and THF cosolvent was the highest and in membrane prepared with 21% PES concentration in NMP solvent the flux rate was the lowest recorded. Furthermore, the membrane hydraulic resistance of 21% PES concentration in NMP prepared membrane was observed to be the highest. The tensile strength of 21% PES concentration in DMF prepared membrane was the lowest and surprisingly the tensile strength of 21% PES concentration in NMP and THF cosolvent was somewhat closest to the 21% PES concentration in NMP prepared membrane. The results indicated that the membrane prepared by solvent mixture of NMP and THF had better water flux performance and better strength as compared to other membranes.

Data Availability

The doc file data used to support the findings of this study are included within the article.

Conflicts of Interest

The authors declare that they have no conflicts of interest.

Acknowledgments

The authors would like to thank School of Chemical and Material Engineering, School of Mechanical and Manufacturing Engineering NUST Islamabad, and Chemical Engineering Department of COMSATS, Lahore. The authors would like to thank Mr. Shams Din (Late) and Mr. Zafar Iqbal of SCME NUST for facilitating the SEM analyses and contact angle measurements, respectively. Thanks are due to Dr. Tahir A. Baig and Ms. Shakira for allowing measuring pure water flux in their lab. Dr. Nasir M. Ahmad acknowledges the support of Higher Education Commission (HEC), National Program for Universities (NRPU), Project nos. 3526 and 3620, for supporting the research work.

References

[1] B. Van Der Bruggen, C. Vandecasteele, T. Van Gestel, W. Doyen, and R. Leysen, "A review of pressure-driven membrane processes in wastewater treatment and drinking water production," *Environmental Progress*, vol. 22, pp. 46–56, 2003.

[2] S. Rana, U. Nazar, J. Ali et al., "Improved antifouling potential of polyether sulfone polymeric membrane containing silver nanoparticles: self-cleaning membranes," *Environmental Technology*, vol. 39, no. 11, pp. 1413–1421, 2018.

[3] D. Vial and G. Doussau, "The use of microfiltration membranes for seawater pre-treatment prior to reverse osmosis membranes," *Desalination*, vol. 153, pp. 141–147, 2002.

[4] R. W. Baker, *Membrane Technology and Applications*, 3rd edition, 2012.

[5] W. Sun, J. Liu, H. Chu, and B. Dong, "Pretreatment and membrane hydrophilic modification to reduce membrane fouling," *Membranes (Basel)*, vol. 3, no. 3, pp. 226–241, 2013.

[6] E. A. Moschou and N. A. Chaniotakis, "Chapter 19 - Ion-partitioning membranes as electroactive elements for the development of a novel cation-selective CHEMFET sensor system," in *Membrane Science and Technology*, D. Bhattacharyya and D. A. Butterfield, Eds., pp. 393–413, Elsevier, 2003.

[7] I. Munnawar, S. S. Iqbal, M. N. Anwar et al., "Synergistic effect of Chitosan-Zinc Oxide Hybrid Nanoparticles on antibiofouling and water disinfection of mixed matrix polyethersulfone nanocomposite membranes," *Carbohydrate Polymers*, vol. 175, pp. 661–670, 2017.

[8] *Processing Guide for Polymer Membranes*, Solvay, 2015.

[9] K. Yadav, K. Morison, and M. P. Staiger, "Effects of hypochlorite treatment on the surface morphology and mechanical properties of polyethersulfone ultrafiltration membranes," *Polymer Degradation and Stability*, vol. 94, no. 11, pp. 1955–1961, 2009.

[10] B. Pellegrin, R. Prulho, A. Rivaton et al., "Multi-scale analysis of hypochlorite induced PES/PVP ultrafiltration membranes degradation," *Journal of Membrane Science*, vol. 447, pp. 287–296, 2013.

[11] C. M. Hansen, "50 Years with solubility parameters—Past and future," *Progress in Organic Coatings*, vol. 51, no. 1, pp. 77–84, 2004.

[12] Y. S. Kang, B. Jung, and U. Y. Kim, "Polymeric dope solution for use in the preparation of an integrally skinned asymmetric membrane," 1998, Google Patents.

[13] V. Laninovic, "Relationship between type of nonsolvent additive and properties of polyethersulfone membranes," *Desalination*, vol. 186, pp. 39–46, 2005.

[14] J. Wijmans, J. Baaij, and C. Smolders, "The mechanism of formation of microporous or skinned membranes produced by immersion precipitation," *Journal of Membrane Science*, vol. 14, no. 3, pp. 263–274, 1983.

[15] D. M. Koenhen, M. H. V. Mulder, and C. A. Smolders, "Phase separation phenomena during the formation of asymmetric membranes," *Journal of Applied Polymer Science*, vol. 21, no. 1, pp. 199–215, 1977.

[16] H. Bokhorst, F. W. Altena, and C. A. Smolders, "Formation of asymmetric cellulose acetate membranes," *Desalination*, vol. 38, pp. 349–360, 1981.

[17] P. Van De Witte, P. J. Dijkstra, J. W. A. Van Den Berg, and J. Feijen, "Phase separation processes in polymer solutions in relation to membrane formation," *Journal of Membrane Science*, vol. 117, no. 1, pp. 1–31, 1996.

[18] M. Ulbricht, "Advanced functional polymer membranes," *Polymer*, vol. 47, no. 7, pp. 2217–2262, 2006.

[19] H. J. Kim, R. K. Tyagi, A. E. Fouda, and K. Jonasson, "The kinetic study for asymmetric membrane formation via phase-inversion process," *Journal of Applied Polymer Science*, vol. 62, no. 4, pp. 621–629, 1996.

[20] Q.-Z. Zheng, P. Wang, Y.-N. Yang, and D.-J. Cui, "The relationship between porosity and kinetics parameter of membrane formation in PSF ultrafiltration membrane," *Journal of Membrane Science*, vol. 286, no. 1-2, pp. 7–11, 2006.

[21] M. Amirilargani, E. Saljoughi, T. Mohammadi, and M. R. Moghbeli, "Effects of coagulation bath temperature and polyvinylpyrrolidone content on flat sheet asymmetric polyethersulfone membranes," *Polymer Engineering & Science*, vol. 50, no. 5, pp. 885–893, 2010.

[22] I.-C. Kim, H.-G. Yoon, and K.-H. Lee, "Formation of integrally skinned asymmetric polyetherimide nanofiltration membranes by phase inversion process," *Journal of Applied Polymer Science*, vol. 84, no. 6, pp. 1300–1307, 2002.

[23] A. C. Sun, W. Kosar, Y. Zhang, and X. Feng, "A study of thermodynamics and kinetics pertinent to formation of PVDF membranes by phase inversion," *Desalination*, vol. 309, pp. 156–164, 2013.

[24] J. Mulder, *Basic Principles of Membrane Technology*, Springer Science & Business Media, 2012.

[25] C. A. Smolders, A. J. Reuvers, R. M. Boom, and I. M. Wienk, "Microstructures in phase-inversion membranes. Part 1. Formation of macrovoids," *Journal of Membrane Science*, vol. 73, no. 2-3, pp. 259–275, 1992.

[26] H. Wood and J. Wang, "The effect of polyethersulfone concentration on flat and hollow fiber membrane performance," *Separation Science and Technology*, vol. 28, no. 15-16, pp. 2297–2317, 1993.

[27] B. K. Chaturvedi, A. K. Ghosh, V. Ramachandhran, M. K. Trivedi, M. S. Hanra, and B. M. Misra, "Preparation, Characterization and performance of polyethersulfone ultrafiltration membranes," *Desalination*, vol. 133, no. 1, pp. 31–40, 2001.

[28] B. Torrestiana-Sanchez, R. I. Ortiz-Basurto, and E. Brito-De La Fuente, "Effect of nonsolvents on properties of spinning solutions and polyethersulfone hollow fiber ultrafiltration membranes," *Journal of Membrane Science*, vol. 152, no. 1, pp. 19–28, 1999.

[29] J. R. Hwang, S.-H. Koo, J.-H. Kim, A. Higuchi, and T.-M. Tak, "Effects of casting solution composition on performance of poly(ether sulfone) membrane," *Journal of Applied Polymer Science*, vol. 60, no. 9, pp. 1343–1348, 1996.

[30] A. Rahimpour, S. S. Madaeni, and Y. Mansourpanah, "High performance polyethersulfone UF membrane for manufacturing spiral wound module: Preparation, morphology, performance, and chemical cleaning," *Polymers for Advanced Technologies*, vol. 18, no. 5, pp. 403–410, 2007.

[31] C. Zhou, Z. Hou, X. Lu et al., "Effect of polyethersulfone molecular weight on structure and performance of ultrafiltration membranes," *Industrial & Engineering Chemistry Research*, vol. 49, no. 20, pp. 9988–9997, 2010.

[32] T. Miyano, T. Matsuura, and S. Sourirajan, "Effect of polyvinylpyrrolidone additive on the pore size and the pore size distribution of polyethersulfone (victrex) membranes," *Chemical Engineering Communications*, vol. 119, no. 1, pp. 23–39, 1993.

[33] M. Panar, H. H. Hoehn, and R. R. Hebert, "The nature of asymmetry in reverse osmosis membranes," *Macromolecules*, vol. 6, no. 5, pp. 777–780, 1973.

[34] C. Hansen et al., *Hansen Solubility Parameters*, B. Raton, Ed., CRC Press, 2007.

[35] G. R. Guillen, Y. Pan, M. Li, and E. M. V. Hoek, "Preparation and characterization of membranes formed by nonsolvent induced phase separation: A review," *Industrial & Engineering Chemistry Research*, vol. 50, no. 7, pp. 3798–3817, 2011.

[36] A. Tabriz, M. A. Ur Rehman Alvi, M. B. Khan Niazi et al., "Quaternized trimethyl functionalized chitosan based antifungal membranes for drinking water treatment," *Carbohydrate Polymers*, vol. 207, pp. 17–25, 2019.

[37] H. T. Bhatti et al., "Graphene oxide-PES-based mixed matrix membranes for controllable antibacterial activity against salmonella typhi and water treatment," *International Journal of Polymer Science*, vol. 2018, Article ID 7842148, 12 pages, 2018.

[38] G. Arthanareeswaran and V. M. Starov, "Effect of solvents on performance of polyethersulfone ultrafiltration membranes: Investigation of metal ion separations," *Desalination*, vol. 267, no. 1, pp. 57–63, 2011.

[39] P. Van De Witte, P. J. Dijkstra, J. W. A. Van Den Berg, and J. Feijen, "Phase separation processes in polymer solutions in relation to membrane formation," *Journal of Membrane Science*, vol. 117, no. 1-2, pp. 1–31, 1996.

[40] Y. L. Thuyavan, N. Anantharaman, G. Arthanareeswaran, and A. F. Ismail, "Impact of solvents and process conditions on the formation of polyethersulfone membranes and its fouling behavior in lake water filtration," *Journal of Chemical Technology and Biotechnology*, vol. 91, no. 10, pp. 2568–2581, 2016.

[41] P. Vandezande, X. Li, L. E. M. Gevers, and I. F. J. Vankelecom, "High throughput study of phase inversion parameters for polyimide-based SRNF membranes," *Journal of Membrane Science*, vol. 330, no. 1, pp. 307–318, 2009.

[42] A. Mushtaq, H. B. Mukhtar, and A. M. Shariff, "FTIR study of enhanced polymeric blend membrane with amines," *Research Journal of Applied Sciences, Engineering & Technology*, vol. 7, no. 9, pp. 1811–1820, 2014.

[43] V. Vatanpour, S. S. Madaeni, R. Moradian, S. Zinadini, and B. Astinchap, "Fabrication and characterization of novel antifouling nanofiltration membrane prepared from oxidized multiwalled carbon nanotube/polyethersulfone nanocomposite," *Journal of Membrane Science*, vol. 375, no. 1-2, pp. 284–294, 2011.

[44] E. Arkhangelsky, D. Kuzmenko, and V. Gitis, "Impact of chemical cleaning on properties and functioning of polyethersulfone membranes," *Journal of Membrane Science*, vol. 305, no. 1-2, pp. 176–184, 2007.

[45] H. Susanto and M. Ulbricht, "Characteristics, performance and stability of polyethersulfone ultrafiltration membranes prepared by phase separation method using different macromolecular additives," *Journal of Membrane Science*, vol. 327, no. 1-2, pp. 125–135, 2009.

[46] N. Biliškov and G. Baranović, "Infrared spectroscopy of liquid water–N,N-dimethylformamide mixtures," *Journal of Molecular Liquids*, vol. 144, no. 3, pp. 155–162, 2009.

[47] A. Sharma et al., "Fourier transform infrared spectral study of N,N′-dimethylformamide-water-rhodamine 6G mixture," *Molecular Physics*, vol. 105, no. 1, pp. 117–123, 2007.

[48] J. Stangret and T. Gampe, "Hydration of tetrahydrofuran derived from FTIR spectroscopy," *Journal of Molecular Structure*, vol. 734, no. 1-3, pp. 183–190, 2005.

[49] A. Iqbal, I. Ani, and R. Rajput, "Performance of microwave synthesized dual solvent dope solution and lithium bromide additives on poly(ethersulfone) membranes," *Journal of Chemical Technology and Biotechnology*, vol. 87, no. 2, pp. 177–188, 2012.

[50] M. A. Alaei Shahmirzadi et al., "Tailoring PES nanofiltration membranes through systematic investigations of prominent design, fabrication and operational parameters," *RSC Advances*, vol. 5, no. 61, pp. 49080–49097, 2015.

[51] A. F. Stalder et al., "Low-bond axisymmetric drop shape analysis for surface tension and contact angle measurements of sessile drops," *Colloids and Surfaces A: Physicochemical and Engineering Aspects*, p. 10, 2010.

[52] B. Vatsha, J. C. Ngila, and R. M. Moutloali, "Preparation of antifouling polyvinylpyrrolidone (PVP 40K) modified polyethersulfone (PES) ultrafiltration (UF) membrane for water purification," *Physics and Chemistry of the Earth, Parts A/B/C*, vol. 67-69, pp. 125–131, 2014.

[53] M. Omidvar et al., "Preparation and characterization of poly (ethersulfone) nanofiltration membranes for amoxicillin removal from contaminated water," *Journal of Environmental Health Science and Engineering*, vol. 12, p. 18, 2014.

[54] M.-J. Han and S.-T. Nam, "Thermodynamic and rheological variation in polysulfone solution by PVP and its effect in the preparation of phase inversion membrane," *Journal of Membrane Science*, vol. 202, pp. 55–61, 2002.

[55] M. I. Mustaffar, A. F. Ismail, and R. M. Illias, "Study on the effect of polymer concentration on hollow fiber ultrafiltration membrane performance and morphology," p. 12, 2013.

[56] K. Kimmerle and H. Strathmann, "Analysis of the structure-determining process of phase inversion membranes," *Desalination*, vol. 79, no. 2, pp. 283–302, 1990.

[57] J.-H. Kim and K.-H. Lee, "Effect of PEG additive on membrane formation by phase inversion," *Journal of Membrane Science*, vol. 138, no. 2, pp. 153–163, 1998.

[58] S. Velu, G. Arthanareeswaran, and L. Muruganandam, "Effect of solvents on performance of polyethersulfone ultrafilteration membranes for separation of metal ions," *International Journal of Chemical and Analytical Science*, 2011.

[59] Y. L. Thuyavan et al., "Preparation and characterization of TiO2-sulfonated polymer embedded polyetherimide membranes for effective desalination application," *Desalination*, vol. 365, pp. 355–364, 2015.

[60] M. G. Buonomenna, *Advanced Materials for Membrane Preparation*, 2012.

[61] A. Figoli et al., "Towards non-toxic solvents for membrane preparation: A review," *Green Chemistry*, vol. 16, no. 9, pp. 4034–4059, 2014.

[62] B. Stefan, B. Marius, and B. Lidia, "Influence of polymer concentration on the permeation properties of nanofiltration membranes," *New Technologies and Products in Machine Manufacturing Technologies*, pp. 227–232, 2011.

[63] J.-F. Li et al., "Hydrophilic microporous PES membranes prepared by PES/PEG/DMAc casting solutions," *Journal of Applied Polymer Science*, vol. 107, no. 6, pp. 4100–4108, 2008.

[64] C. H. Loh and R. Wang, "Effects of additives and coagulant temperature on fabrication of high performance PVDF/Pluronic F127 blend hollow fiber membranes via nonsolvent induced phase separation," *Chinese Journal of Chemical Engineering*, vol. 20, no. 1, pp. 71–79, 2012.